



Facile Synthesis of luminescent carbon material from yogurt for efficient photocatalytic degradation of methylene blue

Muhammad Ali Bhatti, Aneela Tahira, Aqeel Ahmed Shah, Umair Aftab, Brigitte Vigolo, Amira Khattab, Ayman Nafady, Imran Ali Halepoto, Matteo Tonezzer, Zafar Hussain Ibupoto

► To cite this version:

Muhammad Ali Bhatti, Aneela Tahira, Aqeel Ahmed Shah, Umair Aftab, Brigitte Vigolo, et al.. Facile Synthesis of luminescent carbon material from yogurt for efficient photocatalytic degradation of methylene blue. RSC Advances, 2022, 12 (39), pp.25549-25564. 10.1039/d2ra04749g . hal-03807066

HAL Id: hal-03807066

<https://hal.univ-lorraine.fr/hal-03807066>

Submitted on 9 Oct 2022

HAL is a multi-disciplinary open access archive for the deposit and dissemination of scientific research documents, whether they are published or not. The documents may come from teaching and research institutions in France or abroad, or from public or private research centers.

L'archive ouverte pluridisciplinaire **HAL**, est destinée au dépôt et à la diffusion de documents scientifiques de niveau recherche, publiés ou non, émanant des établissements d'enseignement et de recherche français ou étrangers, des laboratoires publics ou privés.

Facile Synthesis of luminescent carbon material from yogurt for efficient photocatalytic degradation of methylene blue

Muhammad Ali Bhatti^a, Aneela Tahira^b, Aqeel Ahmed Shah^c, Umair Aftab^c, Brigitte Vigolo^d, Amira R. Khattabⁱ, Ayman Nafady^g, Imran Ali Halepoto^h, Matteo Tonezzer^f, Zafar Hussain Ibupoto^{b*}

^a Institute of Environmental Sciences, University of Sindh Jamshoro, 76080, Sindh Pakistan

^b Dr. M.A Kazi Institute of Chemistry University of Sindh Jamshoro, 76080, Sindh Pakistan

^c Mehran University of Engineering and Technology, 7680 Jamshoro, Sindh Pakistan

^d Université de Lorraine, CNRS, IJL, F-54000 Nancy, France

^e Department of Metallurgy, NED University of Engineering and Technology, Karachi Pakistan

^f IMEM-CNR, Sede di Trento-FBK, Via alla Cascata 56/C, 38123 Trento, Italy

^g Department of Chemistry, College of Science, King Saud University, Riyadh 11451, Saudi Arabia

^h Institute of Physics University of Sindh Jamshoro, 76080, Sindh Pakistan

ⁱ Department of Pharmacognosy, College of Pharmacy, Arab Academy for Science, Technology and Maritime Transport, Alexandria 1029, Egypt

***Corresponding authors:** Zafar Hussain Ibupoto & Aneela Tahira

Email: zaffar.ibhupoto@usindh.edu.pk; aneelatahira80@gmail.com

Abstract

The present study is focused on yogurt as a simple, inexpensive, abundant and green source for the preparation of luminescent carbon material for enhancing photodegradation of methylene blue (MB). This study introduces an ecological and sustainable approach to large-scale production of carbon material using direct thermal annealing of yogurt in muffle furnace. The size of as prepared carbon material is around 200-300 nm. The particle size distribution was also studied and an average particle of 355 nm was measured. The material exhibits clear luminescence under the illumination with ultraviolet light. The synthesized carbon material shows an outstanding degradation functionality of MB under the irradiation of ultraviolet (UV) light. The degradation of MB was studied in aqueous media. Various dye degradation parameters such as initial dye concentration, catalyst dose, pH of dye solution and scavenger effects have been investigated. The optimum MB concentration was found to be 2.3×10^{-5} M with degradation efficiency of 94.8%. The degradation was highly enhanced at pH 11 with a degradation efficiency of 98.11%. The degradation of MB under highly alkaline condition was mainly governed by the high amount of hydroxyl radicals. Furthermore, the scavenger study confirmed that the hydroxyl radicals were mainly involved in the degradation process. The degradation kinetics of MB followed a first order kinetics with large values of rate constant. The reusability was also studied to ensure the stability of as prepared carbon material during the degradation of MB. The preparation of carbon material with efficient photosensitivity for the degradation of organic dyes from yogurt shows a green and innovative methodology. Therefore, it can be of great interest for the future studies related to energy and environmental applications.

Keywords: yogurt, Carbon material, Methylene blue, Aqueous solution

1. Introduction

Recently, the synthesis of nanostructured materials based on biomass assisted has received a significant attention by the researchers around the world. In this preparation, it is mainly depending on biomolecules which chemically reacts under mild reaction conditions in the absence of toxic chemicals ^[1-3]. In the biosynthesis, the plants and extracts, animals, microorganisms, viruses, DNA and proteins are widely used ^[4-12]. The superiority of biosynthesis to that chemical and physical methods can be described in terms of green aspects for no toxicity to our environment, low cost in terms of use of pressure and energy during synthesis, and nanostructured materials have an excellent biocompatibility, stability and homogeneity ^[2, 13-16]. Therefore, bio-mediated preparation of nanostructured materials is increasingly getting preference. The biosynthesis based nanostructured materials have been studied for various energy conversion systems ^[2, 5, 7].

Wastewater treatment is a very critical problem for clean environment. Wastewater from different industries such as textiles, leather tanning, cosmetics and food is associated with a wide range of synthetic dyes. These dyes are the main water pollution factor and a serious threat to the aquatic life and our environment ^[17, 18]. Methylene blue is extensively used for dyeing fabrics, but it causes prolonged toxic effects on the human body. The most observed adverse effects of methylene blue for human health are allergies, mental disorders, dermatitis, cancer and heart diseases ^[19,20]. Therefore, it is highly important to develop low-cost, simple, and environmentally friendly technologies that allow efficient degradation of methylene blue.

Photocatalysis is considered a highly efficient technology for the degradation of dyes compared to other methodologies, including chemical, physical and biological methods ^[21-25]. For this reason, photocatalysis is today defined as the most advanced technology for the degradation of water-soluble synthetic dyes ^[23,26]. The semiconducting material titanium dioxide (TiO₂) has been widely used as a promising photocatalyst ^[27], and photocatalytic applications based on semiconducting materials have received significant attention ever since ^[28-31]. On the other hand, carbon materials such as carbon dots have proved to be excellent for photocatalytic applications due to their advantageous features such as unique internal and external sp² and sp³ hybridized carbon orbitals ^[32]. Carbon dots exhibit numerous hydrophilic functionalities including hydroxyl, carboxyl, epoxides etc. These properties of carbon dots enable them to be dispersed very well in polar solvents ^[33]. Furthermore, carbon dots exhibit attractive physical and chemical characteristics such as significant luminescence, chemical inertness, limited toxicity, outstanding conductivity, and

water solubility ^[34]. Carbon dots are prepared using both top-down and bottom-up techniques, including carbonization or pyrolysis ^[35,36], chemical oxidation ^[37], arc discharge ^[38], laser etching ^[39], microwaves ^[40], and solvothermal/hydrothermal methods ^[41, 42]. In recent times, biosynthesis method is extensively used to produce nano-sized carbon materials and for this purpose various biomasses have been used to prepare carbon materials such as chest nuts ^[43], coriander ^[44], lemon peel ^[45], cashew gum ^[46], honey ^[47], orange juice ^[38], orange peels ^[49], radish ^[50], egg ^[51], shrimp ^[52], pitahaya ^[53], milk ^[54], apple juice ^[55], stem of banana plant ^[56], pine apple peel ^[57], citric acid ^[58], corn and strawberry powder ^[59], rosemary leaves ^[60], biomass (glucose, chitin, and chitosan) ^[61] etc. These nano-sized carbon materials have been utilized for biological, energy conversion, and environmental applications ^[35]. The biosynthesis method is simple, inexpensive, environment friendly, and highly desirable for large scale production of carbon-based materials. Currently, carbon dots are widely used for the degradation of synthetic dyes due to their intense light absorption, strong light trapping capacity and minimal charge recombination rate of photogenerated electron-hole pairs ^[62]. An innovative, inexpensive, abundant and environmentally friendly source of material such as yogurt has not so far been reported in the existing scientific literature for the production of luminescent carbon material.

In this study, we prepared an innovative green carbon material by carbonizing yogurt produced at a local dairy as an inexpensive, simple, and abundant source. The morphology, crystalline structure, chemical and optical properties of the carbon material were investigated. The green and innovative carbon material was used to degrade methylene blue in aqueous solution under the irradiation of ultraviolet light. Various degradation parameters were studied, such as the photocatalyst dose, the initial dye concentration, and the pH of the dye solution.

2. Experimental Section

2.1. Synthesis of luminescent green and innovative carbon material

The yogurt was purchased in June from a local dairy shop located close to the University of Sindh Jamshoro, Sindh, Pakistan. In typical synthesis of yogurt, the bacteria ferment the lactose sugar into lactic acid. Later lactic acid turns the milk more acidic in nature that helps the proteins to be coagulate. The Yogurt is rich with variety of chemical compounds like fat, protein, water, total solids, and ash. The pH of yogurt was about 4. The yogurt was white more than 80%, 1.5%

greenish and 8.86% yellowish and very coagulated dense material. It was used in the carbonization process without any pre-treatment. A typical preparation process of the luminescent carbon material from yogurt is described below and is shown in Scheme 1. The synthesis process consisted of two steps: (i) carbonization of the yogurt and (ii) separation of the product by filtration. Initially, 40 mL of yogurt was transferred to a 50 mL glass beaker, then carbonized at 200 °C for 2h in a muffle furnace with a ramp rate of 15°C min⁻¹. The 3g of product obtained were dispersed in deionized water and sonicated for 40 minutes, then filtered with a 0.2µm filter membrane. The filtrate was then centrifuged at 5,000 rpm for 30 min to remove the larger carbon particles. Finally, 0.5g of dark brown carbon material were successfully obtained. The morphology of the carbon material was studied by scanning electron microcopy (JSM-5910, JEOL) using a voltage of 20 kV. The Fourier transform infra-red spectroscopy was used to record different vibrational bands (Tensor 27, Bruker Optics FT-IR), and powder X-ray diffraction (Shimadzu-Model Kyoto, Japan) was used to investigate the crystalline structure of the carbon material with Cu/Kα radiation (λ=1.5406 °A) at 45 kV and 45 mA.

2.2. Photocatalytic activity of carbon material prepared from yogurt

The photocatalytic activity of the carbon material was evaluated for the degradation of the MB dye. Initially, different amounts of catalyst (5, 10 and 15 mg) were added to 50 mL of MB dye solution, then stirred to form a homogeneous suspension. Each mixture was stirred in the dark for 30 min before establishing the adsorption-desorption equilibrium between the photocatalyst and the dye solution. Then each dye solution with photocatalyst was transferred to a homemade UV light box and irradiated with UV light to activate the catalyst. The homemade UV box consists of five light emitting diodes (LEDs) with a wavelength of 365 nm and a power of 10 watts. During the irradiation with UV light, 1mL of each dye solution was taken at regular intervals and analyzed using a UV-vis spectrophotometer (Lambda 365, PerkinElmer). The UV-visible absorption spectra were recorded from 200 to 800 nm at different time intervals. The optimal wavelength of 664 nm is related to the intrinsic absorbance wavelength of the MB dye.

The photocatalytic degradation efficiency (%C_{deg}) of the carbon material was calculated using the following equation:

$$\% C_{deg} = \frac{C_0 - C_t}{C_0} \times 100\%, 0 \leq t \leq 6 \quad (1)$$

where C_o and C_t are the MB concentration at the beginning and after reaching the adsorption-desorption equilibrium, respectively. The photodegradation kinetics of the MB dye by means of the carbon material was evaluated through the Langmuir –Hinshelwood equation ^[63] as follows:

$$-Ln\left(\frac{C_o}{C_t}\right)=Kt, 0 \leq t \leq 60 \quad (2)$$

where K_t denotes the rate constant for the pseudo-first order model.

To understand the effect of pH on the degradation process, we adjusted the pH of various MB solutions to 5, 7, 9 and 11. The pH adjustment of the dye solutions was performed with 0.2M NaOH and 0.2M HCl solutions.

2.3. Radical Scavenger experiment

Scavenging experiments were carried out to detect the main reactive species during the photocatalytic decomposition of MB. For this purpose, ascorbic acid ($C_6H_8O_6$), ethylenediamine tetracetate acid disodium ($EDTA-Na_2$) and sodium monohydrate ($NaBH_4$) scavengers were added to the MB solution and the corresponding absorbance spectra were collected. 60 μ of each scavenger at a concentration of 10 mM was added to the MB solution together with 15 mg of photocatalyst. The experiment was conducted for 210 min under the illumination with UV light.

The electrochemical active surface area (ECSA) experiment of as prepared carbon material was performed with cyclic voltammetry at different scan rates. For the electrochemical experiments, we built a three electrode cell of silver-silver chloride ($Ag/AgCl$) filled with 3M KCl electrolytic solution as reference electrode, platinum wire as counter electrode and modified glassy carbon electrode as working electrode. The cleaning of glassy carbon electrode was done with 3 μ m alumina paste solution and silicon paper followed by washing with the deionized water. The glassy carbon electrode was modified with the 5 mg dispersed carbon material ink in the mixture of deionized water and 50 μ L of 5% Nafion solution. Then, 10 μ L (0.2mg) of carbon ink was drop casted on the (0.03 cm²) surface area of glassy carbon electrode and dried with the blow of air at room temperature. Electrochemical impedance spectroscopy (EIS) was carried out with measurement conditions of 50 kHz to 0.1 Hz frequency, amplitude of 5 mV and zero biasing potential. All the electrochemical measurements were done in 2.3×10^{-5} M solution of MB on the Versa potentiostat. The current density was calculated by dividing the measured current with the

surface area of glassy carbon electrode. The obtained EIS spectrum was simulated with Z-view software for the fitted equivalent circuit and estimated charge transfer resistance. The particle size distribution was calculated by dispersing 2 mg of carbon material in 20 mL of deionized water using malvern zetasizer nano (zs).

3. Results and discussion

3.1. Structural characterization of the carbon material prepared from yogurt

The morphology of the carbon material was investigated by scanning electron microscopy (SEM) and SEM images at different magnifications are shown in Figure 1(a,b). The SEM images describe a structure consisting of large sheets (Fig. 1a) composed of small particles, whereas (Fig. 1b), suggests that the material prepared from natural yogurt has graphitic aspects typical of carbon dots. Furthermore, the SEM analysis revealed a uniform size distribution of the carbon material. FTIR analysis was performed to identify the presence of functional groups on the surface of the carbon dots, as shown in Figure 1c. The presence of a large band at 3432 cm^{-1} was assigned to hydroxyl groups (O-H) adsorbed on the surface, while the low peak at 2926 cm^{-1} was attributed to the stretching vibration of the C-H chemical bond. A very weak peak at 2504 cm^{-1} is related to the stretching vibrational frequency of the SH, while the weak peak at 1746 cm^{-1} is attributed to the stretching vibrational frequency of the C=O bond. The peak at 1639 cm^{-1} corresponds to the stretching vibration of C-O and the bending mode of N-H^[64], while the one at 1424 cm^{-1} is related to the stretching frequency of the C-N, N-H, and -COO chemical bonds. These observations confirm that reducing groups including -OH, -NH₂, and -COO are localized on the surface of the carbon dots, in full agreement with various works reported onto fluorescent carbon dots^[65-68].

The UV-visible spectrum of the aqueous solution of carbon material is shown in Figure 1d, where a slight shoulder at 340nm (3.6 eV) related to the $n\text{-}\pi^*$ transition of C=O is visible^[69]. Three characteristic peaks in the 200-400 range are visible, at 233 nm, 281 nm and 340 nm respectively. The absorption bands at 233 and 281 nm come from sp^2 hybrid orbitals of aromatic carbon, belonging to its $\pi\text{-}\pi^*$ transition^[70]. A broad absorption shoulder at 340 nm is related to the C=O bond the revealing $n\text{-}\pi^*$ transition, in good agreement with the reported work^[71, 72]. The UV-visible spectroscopic analysis revealed that the prepared material has characteristics similar to those of carbon dots reported in the works^[71, 72]. The crystalline structure of the material was also

studied through powder XRD technique, and the obtained pattern is shown in Figure 2, in which XRD diffraction peaks at 19.63° , 28.25° , 44.56° , 65.05° and 70.06° are visible. The peak at 19.63° , relative to the (001) planes is hardly visible, while the one at 28.25° , relative to the (002) planes is sharper. Finally, the one at 44.56° , relative to the planes (101), is clear and intense. The presence of these peaks confirms that the material has crystalline characteristics corresponding to graphite, entirely in agreement with the work reported on carbon dots [73]. The inset in Figure 2 shows the image of the luminescent carbon material obtained from yogurt taken with a camera. The carbon material was poured into the quartz glass cuvette, then the UV light was irradiated for 5 min, and then a camera was used to take the picture.

3.2. Photodegradation of methylene blue in aqueous solution under illumination with UV light using carbon-based material

The photocatalytic activity of the carbon-based material was tested for the photodegradation of methylene blue in aqueous solution under the illumination with UV light. Various parameters were studied to evaluate the photocatalytic performance of the prepared carbon-based material, such as the initial dye concentration, the photocatalyst amount, the pH of the MB aqueous solution.

a. Effect of initial MB dye concentration and different doses of photocatalyst

To verify the performance of the photocatalyst obtained from yogurt as a function of the dye concentration, we tested it at two different MB dye concentrations, such as 2.3×10^{-5} M and 0.7×10^{-5} M. Solutions with different amounts of carbon photocatalyst (5, 10 and 15 mg) were irradiated with UV light over time, and the absorption spectra of the dye were compared with those before the photocatalysis process.

First, we studied the effect of different amounts of photocatalyst (5, 10 and 15 mg) on a low concentration of MB (0.7×10^{-5} M) under UV light illumination for 140 min, collecting an absorption spectrum every 20 min, as shown in Figure 3. The absorbance spectra of all three solutions showed a decrease in the MB peak over time and showed almost complete degradation within 140 minutes. These results show that for a low concentration of MB, i.e. 0.7×10^{-5} M, the carbon material prepared from yogurt is exceptionally effective in degrading MB in aqueous solution. We then investigated the performance of various photocatalyst amounts (5, 10 and 15 mg) on a higher concentration of MB dye (2.3×10^{-5} M), as shown in Figure 4. In this case the peak

decreases much more slowly. Furthermore, the solution with 15 mg of catalyst shows the highest degradation efficiency with a value of 94.8 %. This demonstrates that increasing the amount of catalyst significantly affects the photodegradation kinetics. However, the performance of 15 mg of carbon material has a slightly lower degradation efficiency than it does on the lower concentration of MB. This could be attributed to the fact that the 2.3×10^{-5} M concentration could shield the UV light during the process, limiting the number of photons that reach the surface of the carbon material. This would lead to a lower production of electron-hole pairs, to a low amount of oxidizing radicals, and therefore to a lower degradation efficiency.

b. Effect of pH of the MB dye solution

The pH of the dye solution is one of the critical factors on the degradation efficiency ^[74]. Using the MB solution at 2.3×10^{-5} M concentration, considered a more convincing test, 15 mg of photocatalyst were tested at different pH values (5, 7, 9 and 11) under UV light for 160 min. We prepared 100 mL of MB solution at a concentration of 2.3×10^{-5} M, then four solutions with different pH values were obtained by adding an appropriate amount of 0.2 M NaOH or HCl solution. The pH of the dye solution increased to 6.5, 8.8, 10.9 and 12.4 after degradation for the initial pH values of 5, 7, 9 and 11 respectively, indicating the enhancing effect of photocatalytic reaction at different pH values. 15 mg of carbon material was added to each solution at different pH, and the solutions were stirred for 160 min at room temperature as shown in Figure 5. The highest percentage of dye removal was 98.4% for the dye solution with a pH of 11. This can be attributed to the high density of hydroxyl ions under higher alkaline conditions which could act as oxidizing radicals actively involved in the degradation process. Moreover, a possible reason for the higher degradation rate of MB under alkaline conditions is associated to the enhanced dissolving capability of unprotonated MB solution ^[75]. Hydroxyl radicals are produced during photocatalysis via reaction of hydroxide ions with positively charged holes under alkaline pH conditions ^[75]. Hydroxyl radicals strongly support the degradation of MB through the oxidation of hydroxide ions on the surface of the carbon-based material ^[76]. Furthermore, it has been found that the effectiveness of photocatalysis at different pH values is strongly dependent on the nature of the photocatalytic material ^[77]. However, at low pH the relative concentration of hydroxyl ions is lower, therefore a lower degradation rate is observed.

c. Kinetics study of methylene blue degradation

The degradation kinetics of low and high concentration methylene blue have been studied with different amounts of catalyst, as reported in Figure 6. From the first order reaction kinetics, the value of the rate constant (K) can be estimated through the equation $\ln (C_t/C_0) = -kt$. Here, C_t and C_0 are respectively the dye concentration at certain time “t” and at the beginning of the reaction (initial concentration). The rate constant values, reported in Table 1, show that the photodegradation rate is faster at low concentration of MB than at higher concentrations. The MB degradation rate using carbon material obtained from yogurt is comparable or higher than that of many nanostructured materials reported in recent works [78]. The degradation efficiency using 15 mg of carbon material is higher (99.7%) at low MB concentration as shown in Figure 5e, while it is lower but still good (94.8%) at higher concentration, as shown in Figure 5f. These values indicate significantly enhanced photocatalytic properties of the carbon material compared to previous works [79- 81]. Similarly, the study of MB degradation kinetics was also carried out at various pH values of the dye solution (at a concentration of 2.3×10^{-5} M). The degradation kinetics at various pH values are shown in Table 1. In an acidic environment, there is a greater amount of holes which consequently accelerates the degradation kinetics. However, the degradation is relatively slow at low pH due to the possible agglomeration of the carbon material (and therefore the decrease of the catalyst surface) which leads to a poor absorption of UV photons. Additionally, the high density of cationic protons under acidic conditions creates a strong repulsion between the molecules of MB itself, which can reduce the interaction of MB with the catalyst surface, and therefore also the degradation of the dye. In an alkaline environment, there is a high probability of generation of hydroxyl radicals ($\text{HO}\cdot$) which greatly help to degrade the dye. Under highly alkaline conditions, the surface of the carbon material can be negatively charged and promote the adsorption of MB, leading to more efficient photodegradation.

d. Degradation mechanism of MB onto carbon material

The degradation mechanism of MB on carbon material obtained from yogurt under UV light irradiation is shown in Scheme 2. The irradiation with UV light can produce radicals like $\cdot\text{OH}$ and O^{\cdot}_2 which would be actively involved in the degradation of MB resulting in numerous intermediates which eventually decompose into several non-toxic compounds including SO_3 , NO_2 , NH_2 , CH_4 , H_2O and CO_2 . Existing literature shows that the degradation of MB is accompanied by dissociation of the chromophoric structure and decomposition of homo- and heterolytic aromatic

cycles of MB ^[82]. The carbon material is excited during UV light irradiation and as a result radicals might be produced which contribute to the degradation of the MB. This is possible thanks to the availability of numerous electron-hole pairs with adequate energy of the conduction or valence bands, since consequently a high flow of electrons and holes is possible due to their separation at the time of MB degradation under UV light irradiation. Unfortunately, when we tested the photocatalyst under natural sunlight, we found that the degradation performance of MB is limited compared to that achieved under UV light.

e. Scavenger study

The kinetics of MB degradation was also evaluated in the presence of various scavenger and the reaction kinetics followed the pseudo first order mechanism as shown in Figure 8 (a, b). The scavenger agents tested were ascorbic acid, sodium borohydride and ethylenediamine tetraacetate (EDTA). Active radicals such as superoxide radical ions ($\text{O}^{\cdot-}$), hydroxyl radicals (OH^{\cdot}), and photogenerated holes (h^+) have been found to be involved in the degradation process. These selected scavengers are mainly linked to ($\text{O}^{\cdot-}$) and hydroxyl radicals (OH^{\cdot}) ^[83] and the degradation of MB mainly depends on the amount of these oxidizing species, as previously reported in several studies ^[84, 85]. The degradation rate of MB was greatly reduced using EDTA as a scavenger, revealing that hydroxyl radicals play an important role in the degradation of MB under alkaline conditions, as shown in Figure 8c. For understanding the role of as carbon material towards degradation of MB, we have also studied the degradation of MB 2.3×10^{-5} M solution under the illumination of UV light without the use of photocatalyst as shown in Figure 9. The UV-visible absorption spectra suggest the negligible effect on the dye degradation as confirmed from low absorbance value as shown in Figure 9a. The reaction kinetics was further studied as enclosed in Figure 9 (b,c), indicating that the UV light has limited effect on the reaction rate. The degradation efficiency of MB was observed around 6 to 7%, confirming that UV light itself has negligible effect on the dye degradation efficiency as shown in Figure 9d. Therefore, the synthesis of potential of photocatalysts is of immediate need for the efficient wastewater treatment process prior to release of wastewater into the environment from various industrial sector. The stability of as prepared carbon material was also evaluated after three cycles as shown in Figure 10. The initial dye degradation cycle is enclosed in Figure 10a. Figure (b, c) are two reusability cycles for the photodegradation of MB under the illumination of UV light and it can be seen that the prepared

carbon material has significant effectiveness even after three cycles, confirming a good stability of material. The relative degradation efficiency of three cycles are enclosed in Figure 10d. The degradation efficiency of cycle-1, cycle-2 and cycle-3 are 93.3%, 90.2%, 88.3% respectively which is acceptable for a low cost, earth abundant, an innovative and green approach. Furthermore to strengthen the performance of as prepared carbon material, we have analyzed the carbon sample in terms of electrochemical active surface area and impedance spectroscopy as enclosed in Figure 11. Both the electrochemical measurements were done according to our previous work^[86]. The electrochemical active surface area was calculated by cyclic voltammetry at various scan rates as shown in Figure 11a. The linear fitting of current density of anode and cathode sides of CV curves was made and obtained slope value from fitting data was described as the suggested value of electrochemical active surface area (ECSA) as shown in Figure 11b. The obtained result of slope $0.01 \mu\text{cm}^{-2}$ is confirming that the active surface area of carbon material is significant and it evidently supported the efficient degradation performance of carbon material towards MB degradation process. The EIS was also employed to find out the charge transfer of material which could support the performance of as prepared carbon material as enclosed in Figure 11c. The EIS data was simulated and equivalent circuit with well-defined circuit elements is enclosed in the inset of Figure 11c. The circuit elements like solution resistance, carbon material film resistance, constant phase elements and the Warburg constants. The estimated value of charge transfer resistance of carbon material was 50.115 K Ohms from simulation which is close to the value of reported photocatalysts^[87]. Additionally, the semicircle arc of Nyquist plot is another evidence to estimate the material charge transfer resistance value. The EIS study has verified that as prepared carbon material from yogurt exhibits excellent avenues of charge transfer during reaction that could foster the reaction kinetics of MB degradation. Moreover, the particle size distribution of as prepared carbon material was also measured as enclosed in Figure 12. The particle size distribution was experimentally obtained using zetasizer nano (ZS) and the average particle size was found 355 nm. However, the relative concentration of small size particles was low compare to the large particles in the sample. The particle size distribution suggests that the prepared carbon material exhibits nano size, therefore it is shown in the literature that material at nano size has more surface area and consequently enhanced photocatalytic activity was found.

4. Conclusions

In this study, we have synthesized luminescent carbon material from yogurt through a green and innovative method of direct combustion in a muffle furnace. SEM images and XRD patterns showed that the carbon material has similar morphology and structure to those of carbon dots. The UV-visible spectra confirmed that the carbon material exhibits luminescent characteristics. The carbon material was found highly active in the degradation of methylene blue under UV light irradiation. Various aspects of the photocatalyst were studied such as the catalyst dose, the initial dye concentration, and the pH of the dye solution. Furthermore, under alkaline conditions, the MB was degraded even more efficiently. Scavenger studies confirmed that hydroxyl radicals are the potential species for efficient degradation of MB using carbon material prepared from yogurt. The reusability and particle size distribution were also investigated. The production of luminescent carbon material from innovative green natural resources such as yogurt can be of great use for various photocatalytic applications.

Acknowledgement

We extend sincere appreciation to the Researchers Supporting Project (RSP-2022/79) at King Saud University, Riyadh, Saudi Arabia

Conflict of interest

Authors declare no conflict of interest in this research work

5. References

- [1]. A. Rana, K. Yadav and S. Jagadevan, A comprehensive review on green synthesis of nature-inspired metal nanoparticles: Mechanism, application and toxicity. *Journal of Cleaner Production*, 2020, 272, 122880.
- [2]. S. Kaviya, Synthesis, self-assembly, sensing

- methods and mechanism of bio-source facilitated nanomaterials: A review with future outlook. Nano-Structures & Nano-Objects. 2020, **23**, 00498.
- [3]. M. Nasrollahzadeh, M. Sajjadi, S. Iravani and R.S. Varma, Green-synthesized nanocatalysts and nanomaterials for water treatment: Current challenges and future perspectives. *Journal of hazardous materials*, 2021, **401**,123401.
- [4]. K. Dhanaraj and G. Suresh, Conversion of waste sea shell (*Anadara granosa*) into valuable nanohydroxyapatite (nHAp) for biomedical applications. *Vacuum*. 2018, **152**, 222-30
- [5]. W.C. Records, Y. Yoon, J.F. Ohmura, N. Chanut and A.M. Belcher, Virus-templated Pt–Ni (OH) ₂ nanonetworks for enhanced electrocatalytic reduction of water. *Nano Energy*, 2019, **58**,167-174.
- [6]. H. Chandra, P. Kumari, E. Bontempi and S. Yadav, Medicinal plants: Treasure trove for green synthesis of metallic nanoparticles and their biomedical applications. *Biocatalysis and Agricultural Biotechnology*, 2020, **24**, 101518.
- [7]. G. Dong, H. Wang, Z. Yan, J. Zhang, X. Ji, M. Lin, R.A. Dahlgren, X. Shang, M. Zhang and Z. Chen, Cadmium sulfide nanoparticles-assisted intimate coupling of microbial and photoelectrochemical processes: Mechanisms and environmental applications. *Science of The Total Environment*, 2020, **740**, 140080.
- [8]. K. Zhang, X. Wang, C. Long, J. Xu, Z. Jiang, B. Feng, P. Zhang, J. Fei and T. Qing, DNA/RNA chimera-templated copper nanoclusters for label-free detection of reverse transcription-associated ribonuclease H. *Sensors and Actuators B: Chemical*, 2020, **316**, 28072.
- [9]. M. Irfan, P.S. Suprajaa, R. Praveen and B.M. Reddy, Microwave-assisted one-step synthesis of nanohydroxyapatite from fish bones and mussel shells. *Materials Letters*, 2021., **282**,28685.
- [10]. A.R.P. Puthukkara, S.T. Jose and D.S. Lal, Plant mediated synthesis of zero valent iron nanoparticles and its application in water treatment. *Journal of Environmental Chemical Engineering*, 2021, **9** (1).

- [11]. M. Nasrollahzadeh, M. Sajjadi and S.M. Sajadi, Biosynthesis of copper nanoparticles supported on manganese dioxide nanoparticles using *Centella asiatica* L. leaf extract for the efficient catalytic reduction of organic dyes and nitroarenes. *Chinese Journal of Catalysis*, 2018, **39**, 109-117.
- [12]. M. Bordbar, N. Negahdar and M. Nasrollahzadeh, Melissa *Officinalis* L. leaf extract assisted green synthesis of CuO/ZnO nanocomposite for the reduction of 4-nitrophenol and Rhodamine B. *Separation and Purification Technology*, 2018, **191**, 295-300.
- [13]. J.K. Park, E.J. Rupa, M.H. Arif, L.F. Li, G. Anandapadmanaban, J.P. Kang, M. Kim, J.C. Ahn, R. Akter, D.C. Yang and S.C. Kang, Synthesis of zinc oxide nanoparticles from *Gynostemma pentaphyllum* extracts and assessment of photocatalytic properties through malachite green dye decolorization under UV illumination-A Green Approach. *Optik*, 2021, **239**, 166249.
- [14]. N. Sarwar, U.B. Humayoun, M. Kumar, S.F.A. Zaidi, J.H. Yoo, N. Ali, D.I. Jeong, J.H. Lee and D.H. Yoon, Citric acid mediated green synthesis of copper nanoparticles using cinnamon bark extract and its multifaceted applications. *Journal of Cleaner Production*, 2021, **292**, 125974.
- [15]. M. Nasrollahzadeh, M. Sajjadi, J. Dadashi and H. Ghafuri, Pd-based nanoparticles: Plant-assisted biosynthesis, characterization, mechanism, stability, catalytic and antimicrobial activities. *Advances in colloid and interface science*, 2020, **276**, 102103.
- [16]. T. Parandhaman, M.D. Dey, and S.K. Das, S.K. Biofabrication of supported metal nanoparticles: exploring the bioinspiration strategy to mitigate the environmental challenges. *Green Chemistry*, 2019, **21**(20), 5469-5500
- [17]. A.L. Desa, N.H.H. Hairom, L.Y. Ng, C.Y. Ng, M.K. Ahmad and A.W. Mohammad, Industrial textile wastewater treatment via membrane photocatalytic reactor (MPR) in the presence of ZnO-PEG nanoparticles and tight ultrafiltration. *Journal of Water Process Engineering*, 2019, **31**, 100872.
- [18]. C.B. Ong, A.W. Mohammad and L.Y. Ng, Integrated adsorption-solar photocatalytic membrane reactor for degradation of hazardous Congo red using Fe-doped ZnO and Fe-

- doped ZnO/rGO nanocomposites. *Environmental Science and Pollution Research*, 2019, **33**, 33856-33869.
- [19]. N.K. Abdulla, S.I. Siddiqui, N. Tara, A.A. Hashmi and S.A. Chaudhry, Psidium guajava leave-based magnetic nanocomposite γ -Fe₂O₃@GL: A green technology for methylene blue removal from water. *Journal of Environmental Chemical Engineering*, 2019, **6**, 103423.
- [20]. O. Üner, Hydrogen storage capacity and methylene blue adsorption performance of activated carbon produced from *Arundo donax*. *Materials Chemistry and Physics*, 2019, **237**, 121858
- [21]. A. Bhati, S.R. Anand, Gunture, A.K. Garg, P. Khare and S.K. Sonkar, Sunlight-induced photocatalytic degradation of pollutant dye by highly fluorescent red-emitting Mg-N-embedded carbon dots. *ACS Sustainable Chem. Eng.* 2018, **6**, 9246–9256.
- [22]. M. Shanmugam, A. Alsalmeh, A. Alghamdi and R. Jayavel, Enhanced photocatalytic performance of the graphene-V₂O₅ nanocomposite in the degradation of methylene blue dye under direct sunlight. *ACS Appl. Mater. Interfaces* 2015, **7**, 14905–14911.
- [23]. P. Khare, A. Singh, S. Verma, A. Bhati, A.K. Sonker, K.M. Tripathi and S.K. Sonkar, Sunlight-induced selective photocatalytic degradation of methylene blue in bacterial culture by pollutant soot derived nontoxic graphene nanosheets. *ACS Sustainable Chem. Eng.* 2018, **6**, 579–589.
- [24]. X. Li, R. Shen, S. Ma, X. Chen and J. Xie, Graphene-based heterojunction photocatalysts. *Appl. Surf. Sci.* 2018, **430**, 53–107.
- [25]. A.A. Shah, M.A. Bhatti, A. Tahira, A.D. Chandio, I.A. Channa, A.G. Sahito, E. Chalanger, M. Willander, O. Nurand and Z.H. Ibupoto, Facile synthesis of copper doped ZnO nanorods for the efficient photo degradation of methylene blue and methyl orange. *Ceramics International*, 2020, **46**, 9997-10005.
- [26]. J. Wen, J. Xie, X. Chen and X. Li, A review on g-C₃N₄-based photocatalysts. *Appl. Surf. Sci.* 2017, **391**, 72–123.

- [27]. N.L. Stock, J. Peller, K. Vinodgopal and P.V. Kamat, Combinative sonolysis and photocatalysis for textile dye degradation. *Environ. Sci. Technol.* 2000, **34**, 1747–1750.
- [28]. B.C.M. Martindale, G.A.M. Hutton, C.A. Caputo and E. Reisner, Solar hydrogen production using carbon quantum dots and a molecular nickel catalyst. *J. Am. Chem. Soc.* 2015, **137**, 6018–6025.
- [29]. J. Gröttrup, F. Schütt, D. Smazna, O. Lupan, R. Adelung and Y.K. Mishra, Porous ceramics based on hybrid inorganic tetrapodal networks for efficient photocatalysis and water purification. *Ceram. Int.* 2017, **43**, 14915–14922.
- [30]. J. Pan, J. Liu, S. Zuo, U.A. Khan, Y. Yu and B. Li, Structure of Z-scheme CdS/CQDs/BiOCl heterojunction with enhanced photocatalytic activity for environmental pollutant elimination. *Appl. Surf. Sci.* 2018, **444**, 177–186.
- [31]. M.A. Bhatti, A.A. Shah, K.F. Almaani, A. Tahira, A.D. Chandio, M. Willander, O. Nur, A.Q. Mugheri, A.L. Bhatti, B. Waryani, A. Nafady and Z.A. Ibupoto, TiO₂/ZnO Nanocomposite Material for Efficient Degradation of Methylene Blue. *Journal of Nanoscience and Nanotechnology*, 2021, *21*, 2511-2519
- [32]. X. Xu, R. Ray, Y. Gu, H.J. Ploehn, L. Gearheart, K. Raker and W.A. Scrivens, Electrophoretic Analysis and Purification of Fluorescent Single-Walled Carbon Nanotube Fragments. *Journal of the American Chemical Society*, 2004, **40**, 12736- 12737.
- [33]. Y. Cheng, M. Bai, J. Su, C. Fang, H. Li, J. Chen and J. Jiao, Synthesis of fluorescent carbon quantum dots from aqua mesophase pitch and their photocatalytic degradation activity of organic dyes. *Journal of Materials Science & Technology*, 2019, **8**, 1515-1522.
- [34]. A. Yadav, L. Bai, Y. Yang, J. Liu, A. Kaushik, G.J. Cheng, L. Jiang, L. Chi and Z. Kang, Lasing behavior of surface functionalized carbon quantum dot/RhB composites. *Nanoscale*, 2017, **16**, 5049-5054.
- [35]. P. Namdari, B. Negahdari and A. Eatemadi, Synthesis, properties and biomedical applications of carbonbased quantum dots: An updated review. *Biomedicine & Pharmacotherapy*, 2017, **87**, 209-222.

- [36]. J. Di, J. Xia, Y. Ge, H. Li, H. Ji, H. Xu, Q. Zhang, H. Li M. and Li, Novel visible-light-driven CQDs/Bi₂WO₆ hybrid materials with enhanced photocatalytic activity toward organic pollutants degradation and mechanism insight. *Applied Catalysis B: Environmental*, 2015, 168-169, 51-61.
- [37]. X. Zhang, M. Jiang, N. Niu, Z. Chen, S. Li, S. Liu and J. Li, Natural-Product-Derived Carbon Dots: From Natural Products to Functional Materials. *ChemSusChem*, 2018, **1**, 11-24.
- [38]. P. Miao, K. Han, Y. Tang, B. Wang, T. Lin and W. Cheng, Recent advances in carbon nanodots: synthesis, properties and biomedical applications. *Nanoscale*, 2015, **5**, 1586-1595.
- [39]. S. Dey, A. Govindaraj, K. Biswas and C.N.R. Rao, Luminescence properties of boron and nitrogen doped graphene quantum dots prepared from arc-discharge-generated doped graphene samples. *Chemical Physics Letters*, 2014, 595-596, 203-208.
- [40]. L. Cao, X. Wang, M.J. Meziani, F. Lu, H. Wang, P.G. Luo, Y. Lin, B.A. Harruff, L.M. Veca, D. Murray S.Y. and Xie, Carbon Dots for Multiphoton Bioimaging. *Journal of the American Chemical Society*, 2007, **37**, 11318-11319.
- [41]. H. Li, Z. Kang, Y. Liu and S.T. Lee, Carbon nanodots: synthesis, properties and applications. *Journal of Materials Chemistry*, (2012), 22(46), 24230-24253.
- [42]. S. Sahu, B. Behera, T.K. Maiti and S. Mohapatra, Simple one-step synthesis of highly luminescent carbon dots from orange juice: application as excellent bio-imaging agents. *Chemical Communications*, 2012, **70**, 8835-8837.
- [43]. Z. Zhan, S. Zhao and M. Xue, Green preparation of fluorescent carbon dots from water chestnut and its application for mutli-colour imaging in living cells. *Dig. J. Nanomater. Bios.* 2017, **12**, 555–564.
- [44]. A. Sachdev and P. Gopinath, Green synthesis of multi-functional carbon dots from coriander leaves and their potential application as anti-oxidants, sensors and bio-imaging. *Analyst*, 2015, **140**, 4260–4269.

- [45]. A. Tyagi, K.M. Tripathi, N. Singh, S. Choudhary and R.K. Gupta, Green synthesis of carbon quantum dots from lemon peel waste: application in sensing and photo catalysis. *RSC Adv.* 2016, **6**, 72423–72432.
- [46]. N.R. Pries, C.M.W. Santos, R.R. Sousa, R.C.M. d Paule, P.L.R. Cunha and J.P.A. Feista, Novel and fast microwave- assisted synthesis of carbon quantum dots from cashew gum. *J. Braz. Chem. Soc.* 2015, **26**, 1274–1282.
- [47]. X. Yang, Y. Zhuo, S. Zhu, Y. Luo, Y. Feng and Y. Dou, Novel and green synthesis of high-fluorescent carbon dots originated from honey for sensing and imaging, *Biosens. Bioelectron.* 2014, **60**, 292–298.
- [48]. S. Sahu, B. Behara, T.K. Maiti and S. Mohapatra, Simple one-step synthesis of highly luminescent carbon dots from orange juice: application as excellent bioimaging agents. *Chem. Commun.* 2012, **48**, 8835–8837.
- [49]. A. Prasannan and T. Imae, One-pot synthesis of fluorescent carbon dots from orange waste peels. *Ind. Eng. Chem. Res.* 2013, **52**, 15673–15678.
- [50]. W. Liu, H. Diao, H. Chang, H. Wang, T. Li and W. Wei, Green Synthesis of carbon dots from rose-heart radish and application for Fe³⁺ detection and cell imaging. *Sensor Actuat. B-Chem.* 2017, **241**, 190–198.
- [51]. Q. Ye, F. Yan, Y. Luo, Y. Wang, X. Zhou and L. Chen, Formation of N, S-codoped fluorescent carbon dots from biomass and their application for the selective detection for the selective detection of mercury and iron ion. *Spectrochim. Acta A.* 2017, **173**, 854–862.
- [52]. D.L. D'souza, B. Deshmukh, B.R. Bhamore, K.A. Rawat, N. Lenka and S.K. Kailasa, Synthesis of fluorescent nitrogen-doped carbon dots from dried shrimps for cell imaging and boldine drug delivery system. *RSC Adv.* 2016, **6**, 12169– 12179.
- [53]. V. Arul, T.N.J.I. Edison, Y.R. Lee and M.G. Sethuraman, Biological and catalytic applications of green synthesized fluorescent N-doped carbon dots using *Hylocereus undatus*. *J. Photochem. Photobiol. B.* 2017, **168**, 142–148.
- [54]. L. Wang and H.S. Zhou, Green synthesis of luminescent nitrogen-doped carbon dots from milk and its imaging application. *Anal. Chem.* 2014, **86**, 8902–8905.
- [55]. V.N. Mehta, R.K. Singhal and S.K. Kailasa, One step hydrothermal approach to fabricate carbon dots from apple juice for imaging of mycobacterium and fungal cells. *Sensor Actuat. B-Chem.* 2015, **213**, 434–443.

- [56]. A. Somasundaram, V. Anjugam, J. Velu, S. Gandhi, S. Subramanian, K. Konda Ramasamy and V. Balasubramanian, Highly fluorescent carbon dots from Pseudostem of banana plant: applications as nanosensor and bio-imaging agents. *Sensor Actuat. B-Chem.* 2017, **252**, 894–900.
- [57]. A. Somasundaram, V. Anjugam, N. Sampathkumar, J. Shanmugapriya, S. Gandhi, S. Subramanian, M. Shanmugam and V. Balasubramanian, Pineapple peel-derived carbon dots: applications as sensor, molecular keypad lock, and memory device. *ACS Omega.* 2018, **3**, 12584–12592.
- [58]. N. Gao, L. Huang, T. Li, J. Song, H. Hu, Y. Liu and S. Ramakrishna, Application of carbon dots in dye-sensitized solar cells: a review *J. Appl. Polym. Sci.*, 2020, **137**, 1-11.
- [59]. Y. Zhao, J. Duan, B. He, Z. Jiao and Q. Tang, Improved charge extraction with n-doped carbon quantum dots in dye-sensitized solar cells. *Electrochim. Acta*, 2018, **282**, 255-262.
- [60]. B. Rezaei, N. Irannejad, A.A. Ensafi and N. Kazemifard, The impressive effect of eco-friendly carbon dots on improving the performance of dye-sensitized solar cells. *Sol. Energy*, 2019, 182, 412-419.
- [61]. J. Briscoe, A. Marinovic, M. Sevilla, S. Dunn and M. Titirici, Biomass-derived carbon quantum dot sensitizers for solid-state nanostructured solar cells *Angew. Chem. - Int. Ed.* 2015, **54**, 4463-4468.
- [62]. U. Abd Rani, L.Y. Ng, C.Y. Ng, E. Mahmoudi, Y.S. Ng and , A.W. Mohammad, Sustainable production of nitrogen-doped carbon quantum dots for photocatalytic degradation of methylene blue and malachite green. *Journal of Water Process Engineering*, (2021), 40, 101816
- [63]. M.A. Bhatti, K.F. Almaani, A.A. Shah, A. Tahira, A.D. Chandio, A.Q. Mugheri, and Z.A. Ibupoto, . Low Temperature Aqueous Chemical Growth Method for the Doping of W into ZnO Nanostructures and Their Photocatalytic Role in the Degradation of Methylene Blue. *Journal of Cluster Science*, 2021, 1-12.
- [64]. Y. Yang, J. Cui, M. Zheng, C. Hu, S. Tan, Y. Xiao, Q. Yang and Y. Liu, Y. One-step synthesis of amino-functionalized fluorescent carbon nanoparticles by hydrothermal carbonization of chitosan,” *Chemical Communications*, 2012, **48**, 380–382,

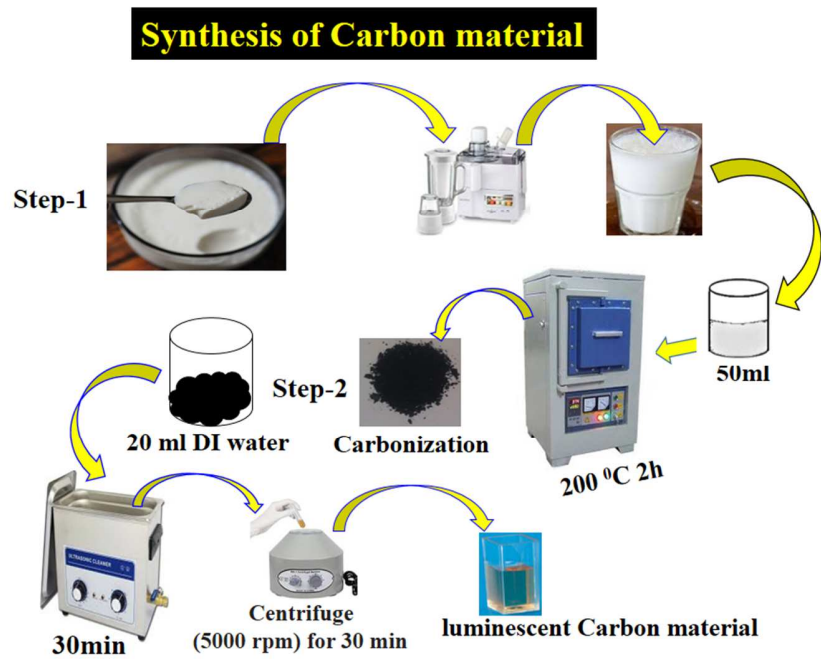
- [65]. H. Tetsuka, R. Asahi, A. Nagoya, K. Okamoto, I. Tajima, R. Ohta and A. Okamoto, Optically tunable amino-functionalized graphene quantum dots,” *Advanced Materials*, 2012, **24**, 5333–5338, 2012.
- [66]. S. H. Jin, D. H. Kim, G. H. Jun, S. H. Hong and S. Jeon, Tuning the photoluminescence of graphene quantum dots through the charge transfer effect of functional groups,” *ACS Nano*, 2013, **7**, 1239–1245.
- [67]. S. Sugiarti and N. Darmawan, Synthesis of fluorescence carbon nanoparticles from ascorbic acid. *Indones. J. Chem.* 2015, **15**, 141-145.
- [68]. Z. Zhang, W. Sun and P. Wu, Highly photoluminescent carbon dots derived from egg white: facile and green synthesis, photoluminescence properties, and multiple applications. *ACS Sustainable Chem. Eng.* 2015, **3**, 1412-1418.
- [69]. G. Eda, Y.Y. Lin, C. Mattevi, H. Yamaguchi, H.A. Chen, I.S. Chen, C.W. Chen and M. Chhowalla, Blue photoluminescence from chemically derived graphene oxide. *Adv. Mater.*, 2010, **22**, 505–509.
- [70]. D.Y. Pan, J.C. Zhang, Z. Li and M.H. Wu, Hydrothermal Route for Cutting Graphene Sheets into Blue-Luminescent Graphene Quantum Dots. *Adv. Mater.* 2010, **22**, 734-738.
- [71]. M. Zheng, Z. G. Xie, D. Qu, D. Li, P. Du, X.B. Jing Z.C. Sun, On-Off-On Fluorescent Carbon Dot Nanosensor for Recognition of Chromium(VI) and Ascorbic Acid Based on the Inner Filter Effect. *ACS Appl. Mater. Interfaces* 2013, **5**, 13242-13247.
- [72]. W.J. Wang, X. Hai, Q.X. Mao, M.L. Chen and J.H. Wang, Polyhedral oligomeric silsesquioxane functionalized carbon dots for cell imaging, *ACS Appl. Mater. Interfaces*, 2015, **7**, 16609–16616
- [73]. T. Wang, A. Wang, R. Wang, Z. Liu, Y. Sun, G. Shan Y. Liu, Carbon dots with molecular fluorescence and their application as a “turn-off” fluorescent probe for ferricyanide detection. *Scientific reports*, 2019, **9**, 1-9.
- [74]. H.P. Jing, C. C. Wang, Y. W. Zhang, P. Wang and R. Li, Photocatalytic degradation of methylene blue in ZIF-8. *RSC Advances* 2014, **4**, 54454–62..

- [75]. U.G. Akpan and B. H. Hameed, Parameters affecting the photocatalytic degradation of dyes using TiO₂-based photocatalysts: A review. *Journal of Hazardous Materials* 2009, **170** (2–3):520–9.
- [76]. L.L.F. Wen, J. Wang, L. Feng, C.G. Lv, Wang and D.F. Li, Structures, photoluminescence, and photocatalytic properties of six new metal-organic frameworks based on aromatic polycarboxylate acids and rigid imidazole-based synthons. *Crystal Growth and Design* 2009, **9**, 3581–9
- [77]. M. N. Chong, B. Jin, C. W. K. Chow and C. Saint, Recent developments in photocatalytic water treatment technology: A review. *Water Research* 2010, **44**, 2997–3027.
- [78]. J. Guo, F. Dong, S. Zhong, B. Zhu, W. Huang S. and Zhang, TiO₂-hydroxyapatite composite as a new support of highly active and sintering-resistant gold nanocatalysts for catalytic oxidation of CO and photocatalytic degradation of methylene blue. *Catal Lett* 2018, **148**, 359–373.
- [79]. A. Singh Vig, A. Gupta and O.P. Pandey, Efficient photodegradation of methylene blue (MB) under solar radiation by ZrC nanoparticles. *Adv Powder Technol* 2018, **29**, 2231–2242.
- [80]. S. Mallakpour and M. Hatami, LDH-VB9-TiO₂ and LDH-VB9-TiO₂/crosslinked PVA nanocomposite prepared via facile and green technique and their photo-degradation application for methylene blue dye under ultraviolet illumination. *Appl Clay Sci* 2018, **163**, 235–248.
- [81]. H.R. Pouretedal, A. Kadkhodaie, Synthetic CeO₂ nanoparticle catalysis of methylene blue photodegradation: kinetics and mechanism. *Chin J Catal* 2010, **31**, 1328–1334.
- [82]. M. Jacob, R. Rajan, M. Aji, G.G. Kurup and A. Pugazhendhi, Bio-inspired ZnS quantum dots as efficient photo catalysts for the degradation of methylene blue in aqueous phase, *Ceram. Int.* 2019, **45**, 4857–4862

- [83]. G. S. Sunil, K.M. Vilas, P.P. Sandip and H.S. Gunvant, Effect of doping parameters on photocatalytic degradation of methylene blue using Ag doped ZnO nanocatalyst, *SN Applied Sciences*. 2020, **2**, 820
- [84]. B. Mondol, A. Sarker, A.M. Shareque, S.C. Dey, M.T. Islam, A.K. Das, S.M. Shamsuddin, M.A.I. Molla and M. Sarker, Preparation of Activated Carbon/TiO₂ Nanohybrids for Photodegradation of Reactive Red-35 Dye Using Sunlight. *Photochem*. 2021, **1** 54–6
-
- [85]. M.A.I. Molla, I. Tateishi, M. Furukawa, H. Katsumata, T. Suzuki and S. Kaneco, Evaluation of Reaction Mechanism for Photocatalytic Degradation of Dye with Self-Sensitized TiO₂ under Visible Light Irradiation. *Open J. Inorg. Non-Met. Mater*. 2017, **7**, 1–7
- [86]. A. J. Laghari, U. Aftab A. Tahira, A. A. Shah, A. Gradone, M. Y. Solangi, A. H. Samo, M. kumar, M. I. Abro, M. W. Akhtar, R. Mazzaro, V. Morandi, A. M. Alotaibi, A. Nafady, A. I. Molina, Z. H. Ibupoto, MgO as promoter for electrocatalytic activities of Co₃O₄–MgO composite via abundant oxygen vacancies and Co²⁺ ions towards oxygen evolution reaction, *Int. Journal of Hydr. Energy*, 2022, **04**,169
- [87]. D. Hartanto, G. Yuhaneke, W. P. Utomo, A. I. Rozafia, Y. Kusumawati, W. Dahani, and Ani Iryani, *RSC Adv*. 2022, **12**, 5665–5676.
- [88]. Z. Zhu, P. Yang, X. Li, M. Luo, W. Zhang, M. Chen and X. Zhou, Green preparation of palm powder-derived carbon dots co-doped with sulfur/chlorine and their application in visible-light photocatalysis. *Spectrochimica Acta Part A: Molecular and Biomolecular Spectroscopy*, 2020, **227**, 117659.
- [89]. A. Aghamali, M. Khosravi, H. Hamishehkar, N. Modirshahla and M.A. Behnajady, Synthesis and characterization of high efficient photoluminescent sunlight driven photocatalyst of N-Carbon Quantum Dots. *Journal of Luminescence*, 2018, **201**, 265-274
- [90]. W. Wang, Y. Ni and Z. Xu, One-step uniformly hybrid carbon quantum dots with high-reactive TiO₂ for photocatalytic application. *Journal of Alloys and Compounds*, 2015, **622**, 303-308.

- [91]. V. Ramar, S. Moothattu and K. Balasubramanian, Metal free, sunlight and white lightbased photocatalysis using carbon quantum dots from *Citrus grandis*: a green way to remove pollution. *Solar Energy*, 2018, **169**, 120-127
- [92]. J. Zhang, X. Zhang, S. Dong, X. Zhou and S. Dong, N-doped carbon quantum dots/TiO₂ hybrid composites with enhanced visible light driven photocatalytic activity toward dye wastewater degradation and mechanism insight. *Journal of Photochemistry and Photobiology A: Chemistry*, 2016, **325**, 104-110.
- [93]. M. Rahbar, M. Mehrzad, M. Behpour, S. Mohammadi-Aghdam and M. Ashrafi, S, N co-doped carbon quantum dots/TiO₂ nanocomposite as highly efficient visible light photocatalyst. *Nanotechnology*, 2019, **30**, 505702.
- [94]. Y. Hou, Q. Lu, H. Wang, H. Li, Y. Zhang and S. Zhang, One-pot electrochemical synthesis of carbon dots/TiO₂ nanocomposites with excellent visible light photocatalytic activity. *Materials Letters*, 2016, **173**, 13-17.
- [95]. Z. Zhang, T. Zheng, J. Xu, H. Zeng and N. Zhang, Carbon quantum dots/Bi₂MoO₆ composites with photocatalytic H₂ evolution and near infrared activity. *Journal of Photochemistry and Photobiology A: Chemistry*, 2017, **346**, 24-31.
- [96]. Y. Cheng, M. Bai, J. Su, C. Fang, H. Li, J. Chen and J. Jiao, Synthesis of fluorescent carbon quantum dots from aqua mesophase pitch and their photocatalytic degradation activity of organic dyes. *Journal of materials science & technology*, 2019, **35**, 1515-1522.
- [97]. M. Saikia, T. Das, N. Dihingia, X. Fan, L.F. Silva and B.K. Saikia, Formation of carbon quantum dots and graphene nanosheets from different abundant carbonaceous materials. *Diamond and Related Materials*, 2020, **106**, 107813.
- [98]. U.R.R.P. Remli and A.A. Aziz, Photocatalytic degradation of methyl orange using Carbon Quantum Dots (CQDs) derived from watermelon rinds. In *IOP Conference Series: Materials Science and Engineering*, 2020, **736**, 042038.
- [99]. T. T. V. Nu, N. H. T. Tran, P.L. Truong, B.T. Phan, M.N.T. Dinh, V.P. Dinh V. Van Tran, Green synthesis of microalgae-based carbon dots for decoration of TiO₂ nanoparticles in enhancement of organic dye photodegradation. *Environmental research*, 2022, **206**, 112631.
- [100]. C. Wang, J. Xu, R. Zhang and W. Zhao, Facile and low-energy-consumption synthesis of dual-functional carbon dots from *Cornus walteri* leaves for detection of p-nitrophenol and

photocatalytic degradation of dyes. *Colloids and Surfaces A: Physicochemical and Engineering Aspects*, 2022, 128351.



11

Scheme 1: Scheme of green and innovative carbon material synthesis process

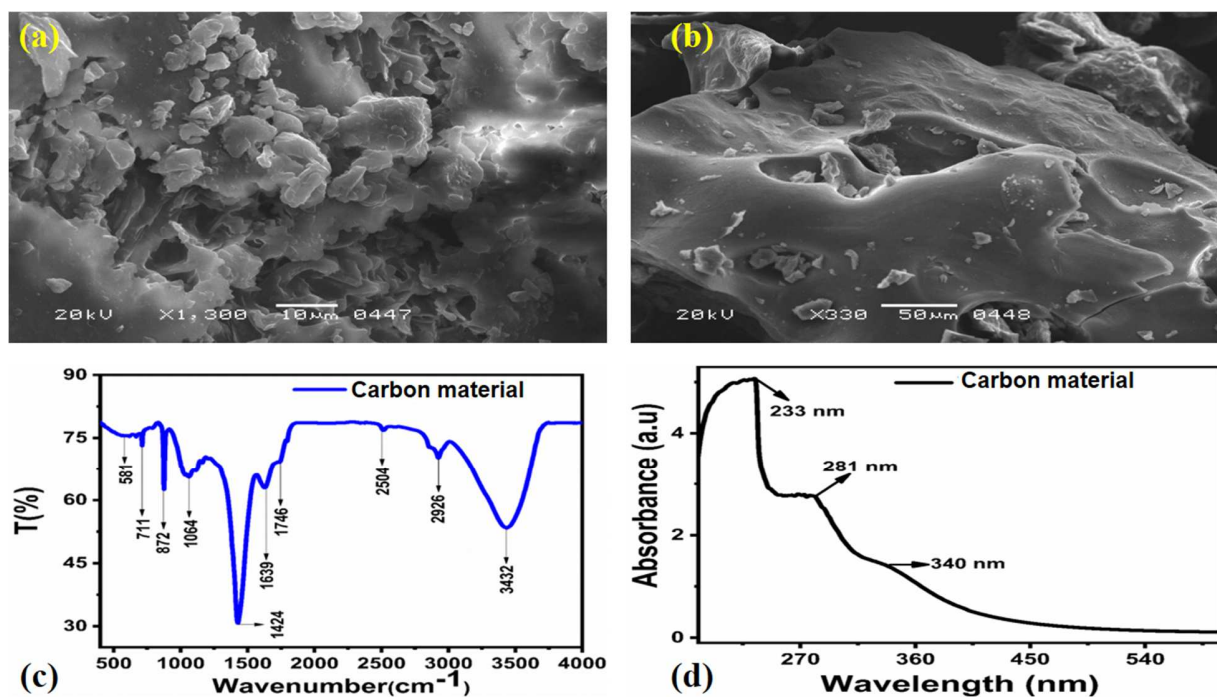


Figure 1(a,b): SEM images green and innovative carbon material at different magnifications, (c) FTIR spectrum of carbon material, (d) UV-visible absorbance spectrum of carbon material

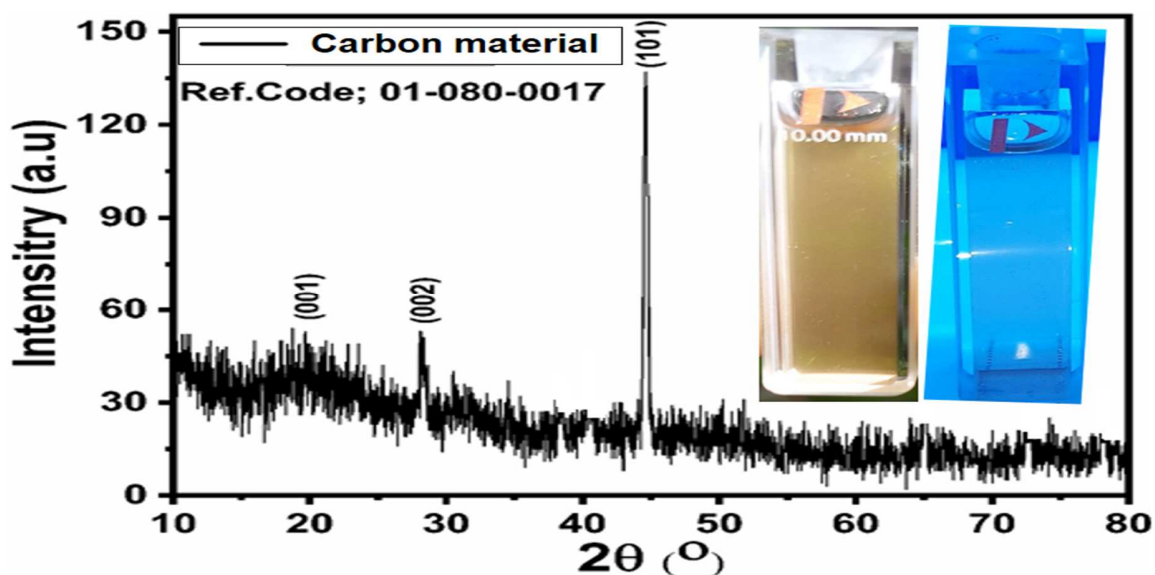


Figure 2: XRD diffraction patterns of carbon material obtained from yogurt, inset shows the luminescent aspects of carbon material

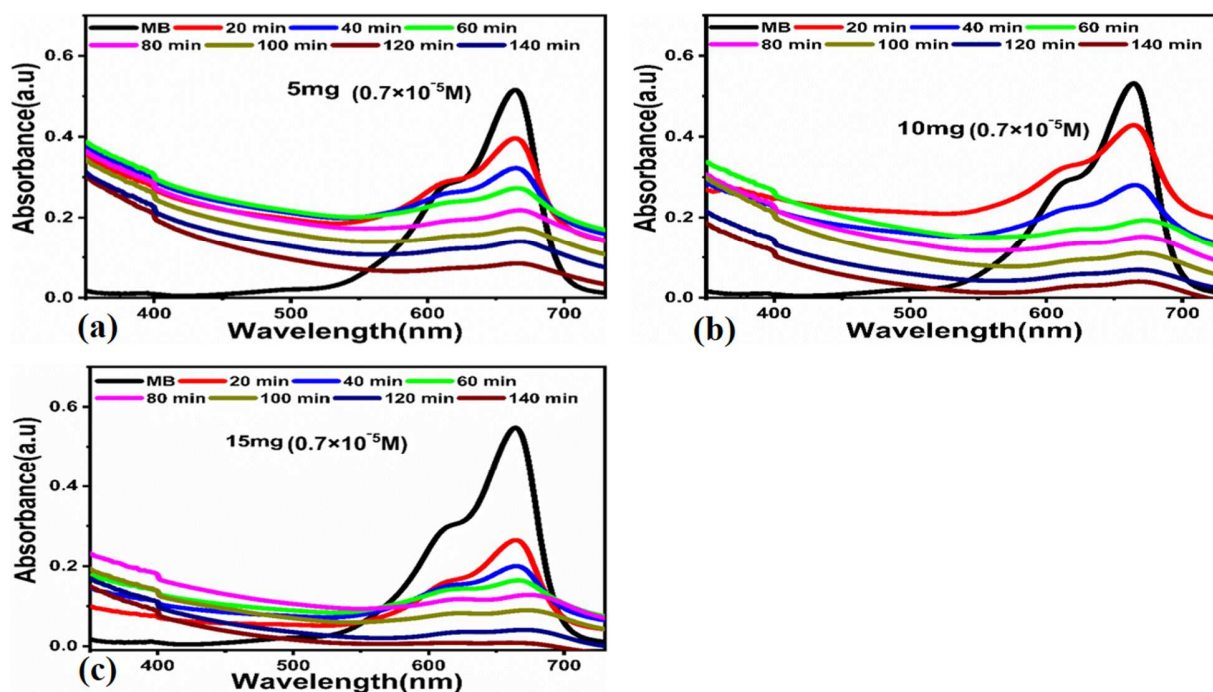


Figure 3: UV-visible absorbance spectra in MB concentration of $0.7 \times 10^{-5} \text{ M}$ for the time interval of 140 minutes under the irradiation of UV light (a) a catalyst dose of 5 mg (b) a catalysts dose of 5 mg (c) a catalyst dose of 5 mg

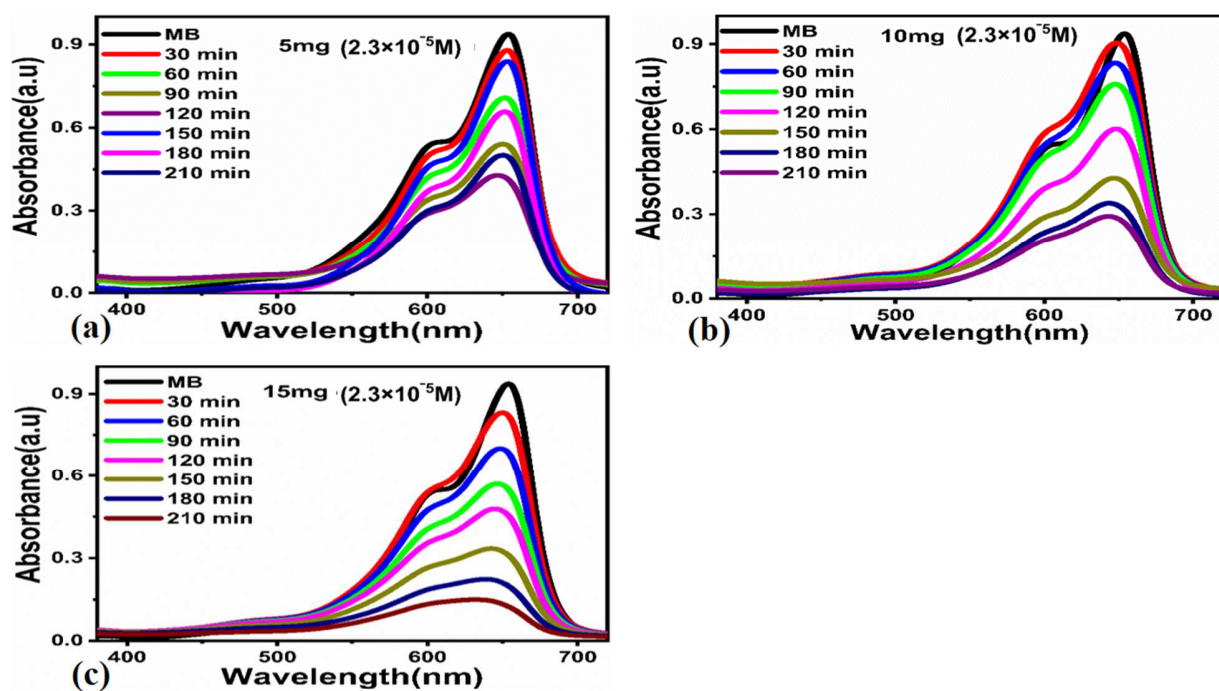


Figure 4: UV-visible absorbance spectra in MB concentration of $2.3 \times 10^{-5} \text{ M}$ for the time interval of 210 minutes under the irradiation of UV light (a) a catalyst dose of 5 mg (b) a catalysts dose of 10 mg (c) a catalyst dose of 15 mg

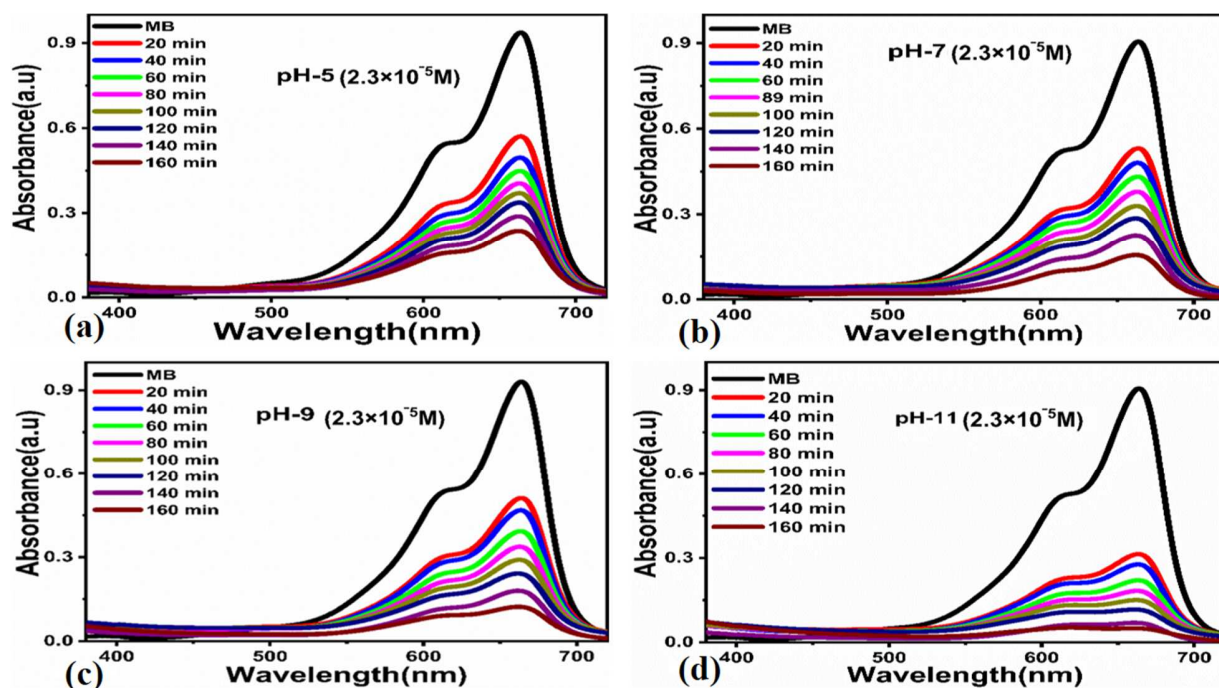


Figure 5: UV-visible absorbance spectra in MB concentration of $2.3 \times 10^{-5} \text{ M}$ at different pH values of dye solution for the time interval of 160 minutes under the irradiation of UV light using catalyst dose of 15 mg (a) pH 5 (b) pH 7 (c) pH 9 (d) pH 11

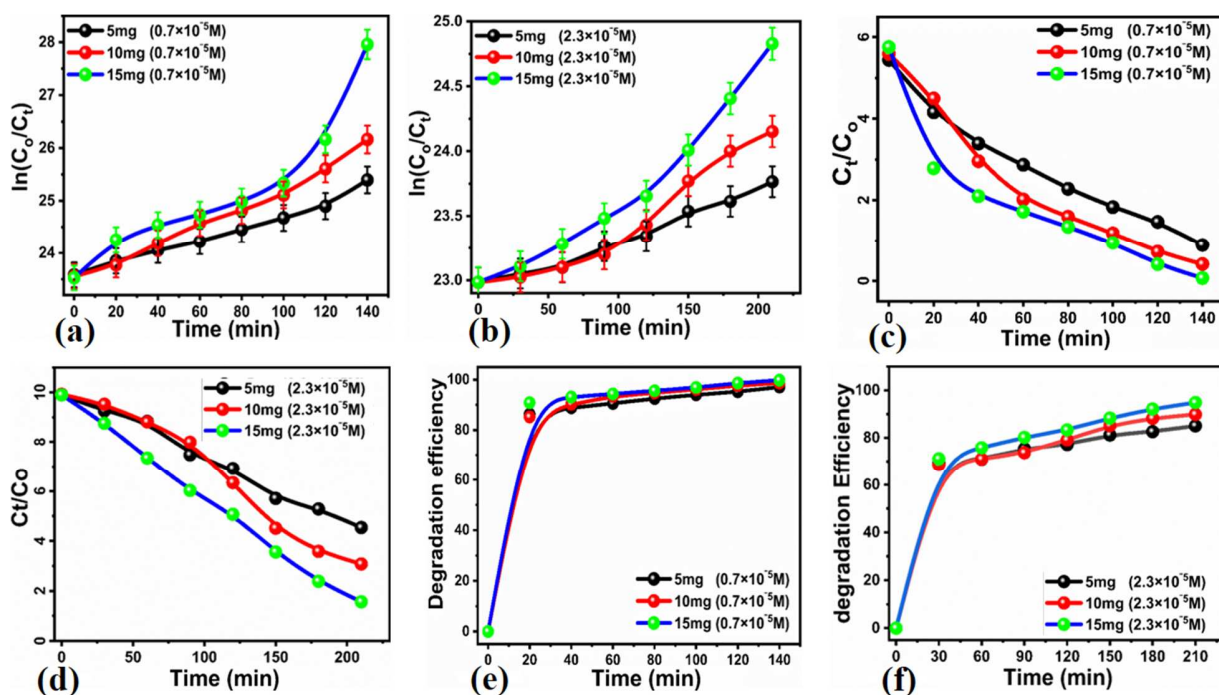


Figure 6: Evaluation of degradation kinetics (a) linear plot of natural logarithm of concentrations like C_0 initial and C_t after certain intervals of time in MB concentration of $0.7 \times 10^{-5} \text{ M}$ with various catalyst doses of 5, 10 and 15 mg for the time interval of 140 minutes (b) linear plot of natural logarithm of concentrations like C_0 initial and C_t after certain intervals of time in MB concentration of $2.3 \times 10^{-5} \text{ M}$ with various catalyst doses of 5, 10 and 15 mg for the time interval of 210 minutes (c) linear plot of concentrations like C_0 initial and C_t after certain intervals of time in MB concentration of $0.7 \times 10^{-5} \text{ M}$ with various catalyst doses of 5, 10 and 15 mg for the time interval of 140 minutes (d) linear plot of concentrations like C_0 initial and C_t after certain intervals of time in MB concentration of $2.3 \times 10^{-5} \text{ M}$ with various catalyst doses of 5, 10 and 15 mg for the time interval of 140 minutes (e) degradation efficiency of MB concentration $0.7 \times 10^{-5} \text{ M}$ with various catalyst doses of 5, 10 and 15 mg for the time interval of 140 minutes (f) degradation efficiency of MB concentration $2.3 \times 10^{-5} \text{ M}$ with various catalyst doses of 5, 10 and 15 mg for the time interval of 210 minutes

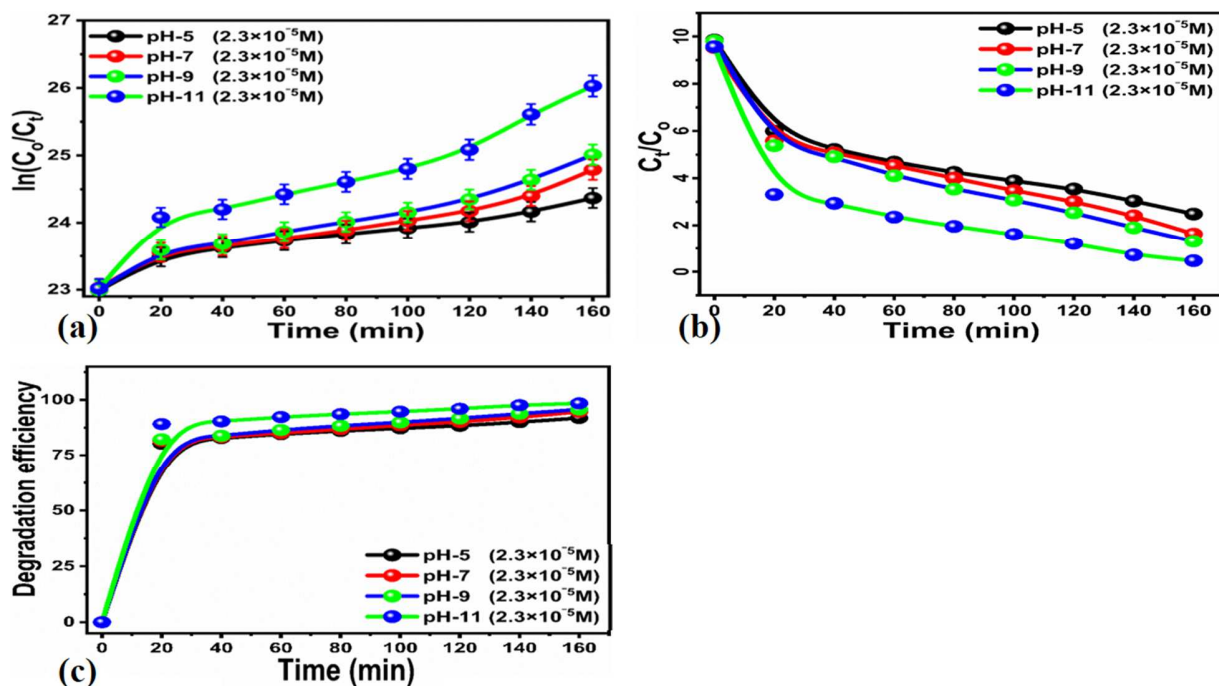
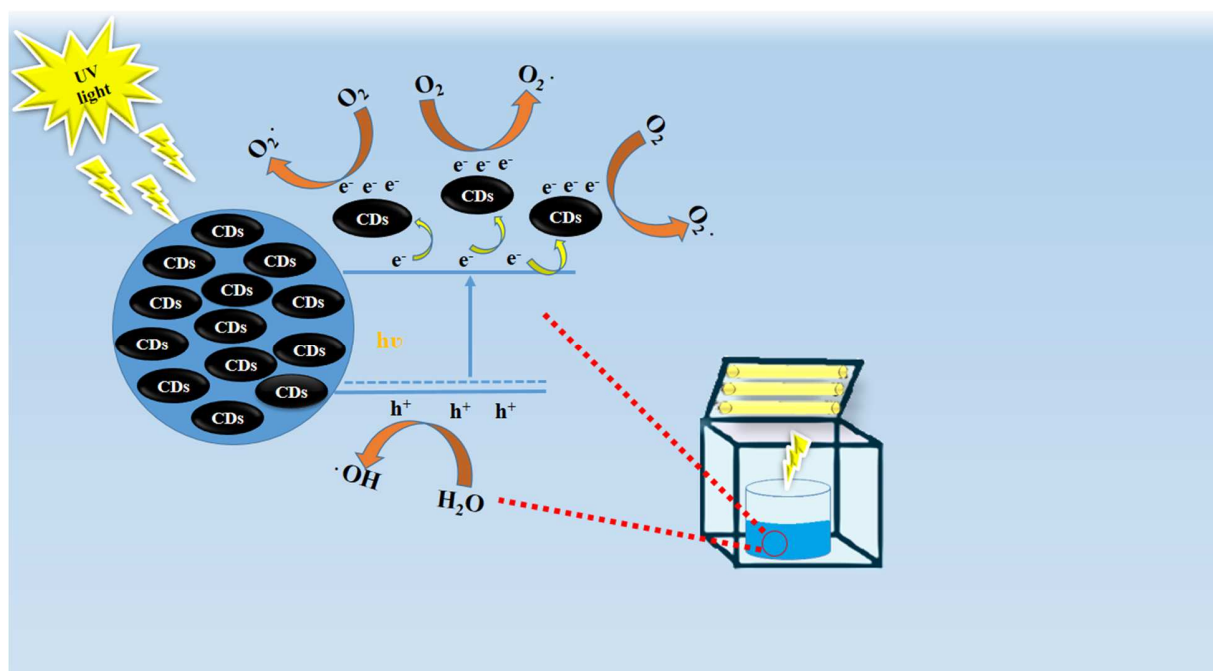


Figure 7: Evaluation of degradation kinetics (a) linear plot of natural logarithm of concentrations like C_0 initial and C_t after certain intervals of time in MB concentration of $2.3 \times 10^{-5} \text{ M}$ with 15 mg for the time interval of 150 minutes for pH values 5, 7, 9 and 11 (b) linear plot of concentrations like C_0 initial and C_t after certain intervals of time in MB concentration of $2.3 \times 10^{-5} \text{ M}$ with various catalyst dose of 15 mg for the time interval of 150 minutes for pH values 5, 7, 9 and 11 (c) degradation efficiency of MB concentration $2.3 \times 10^{-5} \text{ M}$ with catalyst dose of 15 mg for the time interval of 150 minutes for pH values 5, 7, 9 and 11



Scheme 2: Shows the proposed reaction mechanism of MB onto luminescent carbon material prepared from yogurt

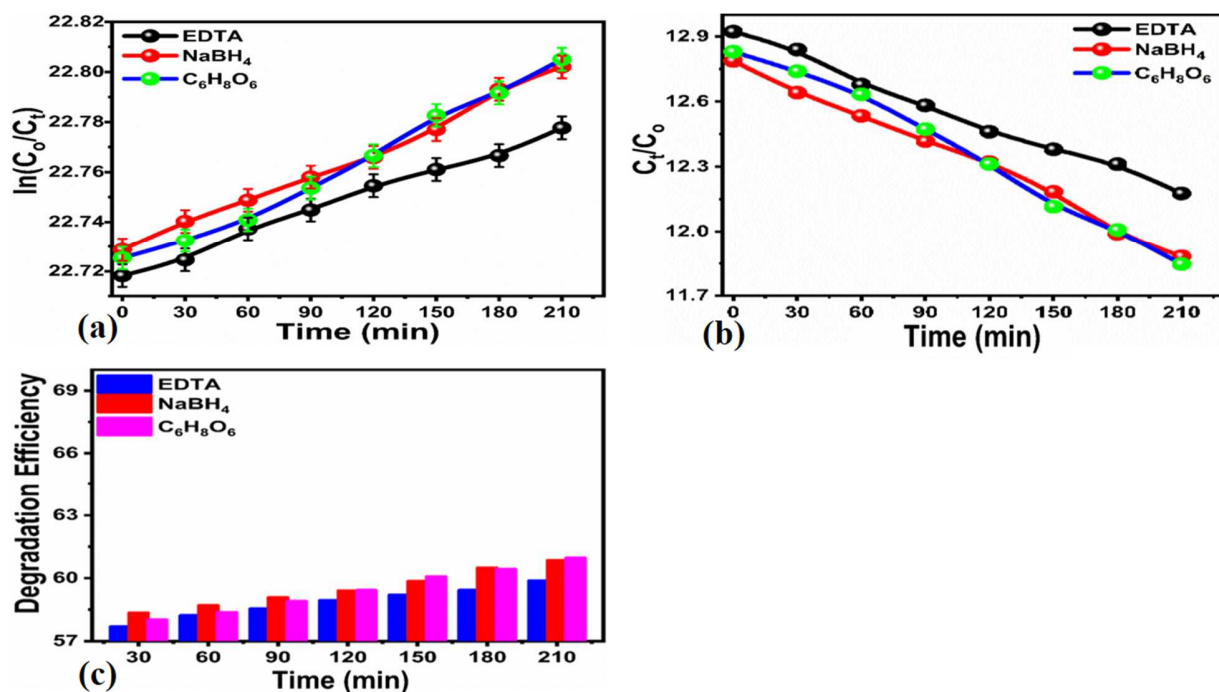


Figure 8: Evaluation of degradation kinetics (a) linear plot of natural logarithm of concentrations like C_0 initial and C_t after certain intervals of time in MB concentration of 2.3×10^{-5} M with 15 mg for the time interval of 210 minutes in the presence of different scavenger (b) linear plot of concentrations like C_0 initial and C_t after certain intervals of time in MB concentration of 2.3×10^{-5} M with a catalyst dose of 15 mg for the time interval of 210 minutes in the presence of different scavenger (c) degradation efficiency of MB under the environment of different scavengers in MB concentration of 2.3×10^{-5} M using a catalyst dose of 15 mg under the irradiation of UV light.

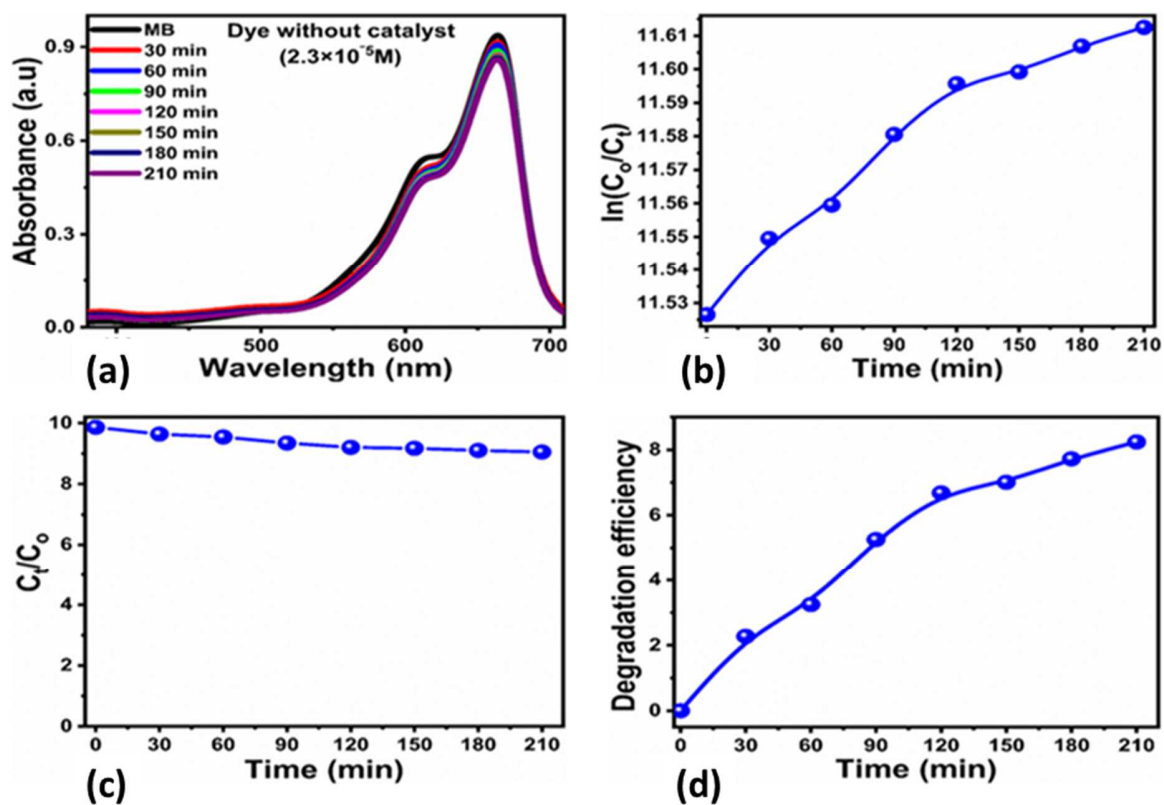


Figure 9: (a) UV-visible absorbance spectra of MB concentration of 2.3×10^{-5} M without the use of photocatalyst for the time interval of 210 minutes under the irradiation of UV light, (b, c) reaction kinetics with the photocatalyst (d) degradation efficiency without the photocatalyst

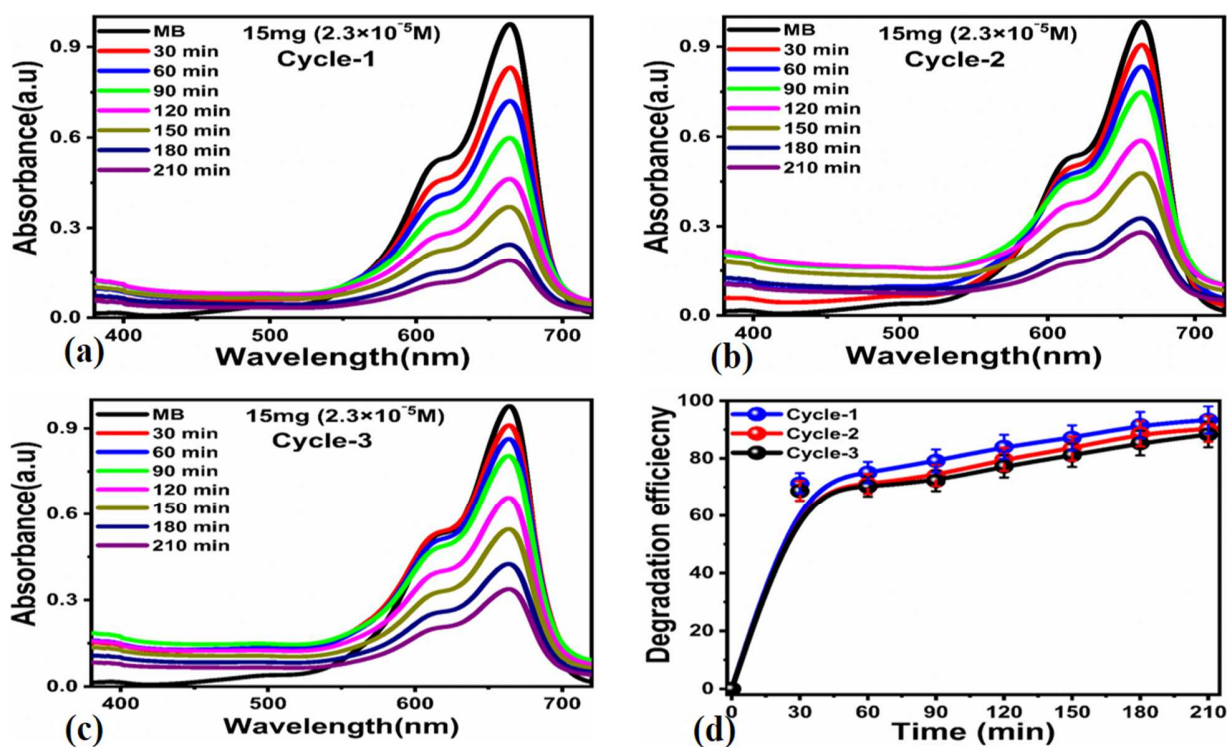


Figure 10: UV-visible absorbance spectra in MB concentration of 2.3×10^{-5} M for understanding the reusability of carbon material for the time interval of 160 minutes under the irradiation of UV light using catalyst dose of 15 mg (a) Cycle-1 (b) cycle-2 (c) cycle-3 (d) %photodegradation efficiency

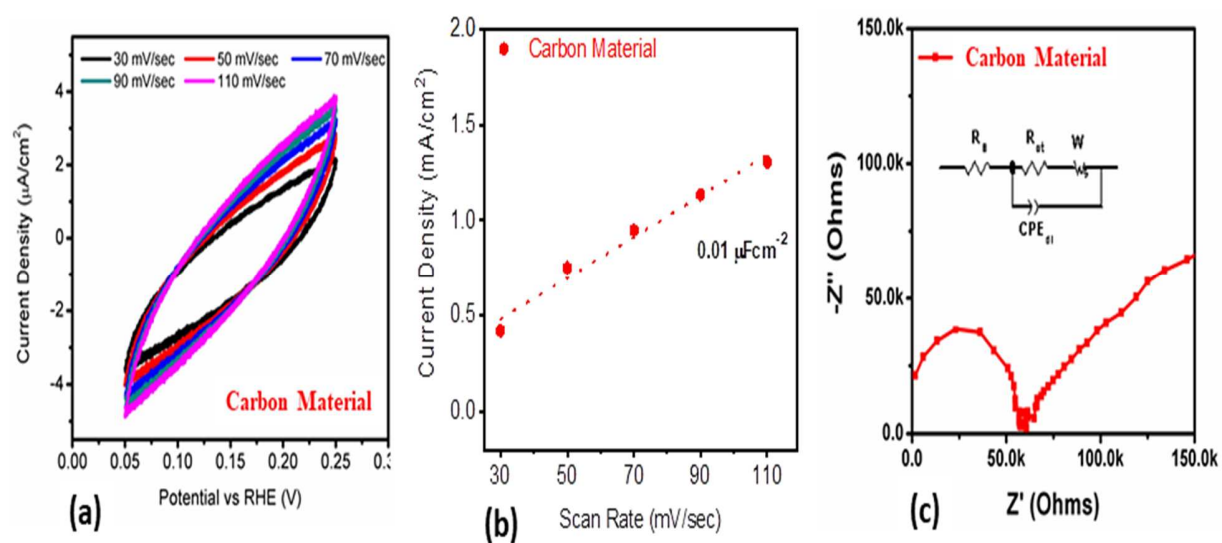


Figure 11: (a) Cyclic voltammetry curves at various scan rates in 2.3×10^{-5} M solution of MB, (b) linear fitting of current density at various scan rate, (c) EIS spectrum of as prepared carbon material in 2.3×10^{-5} M solution of MB

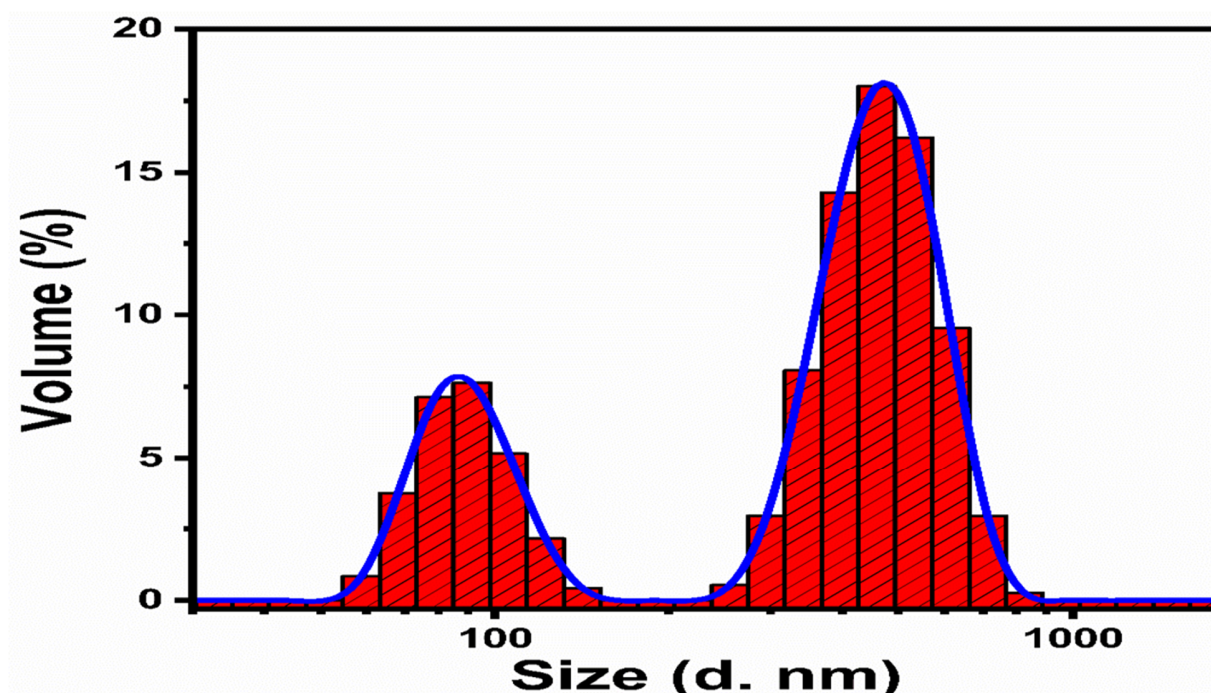


Figure 12: Particle size distribution of as prepared carbon material from yogurt using nano sizer

Table 1: Summary of obtained results with carbon material from yogurt

Sample Dose	Dye con:	Constant (K)	Dye con:	Constant (K)	Scavengers	Constant (K)
5mg	2.3 ×10 ⁻⁵ M	3.83×10 ⁻³ min ⁻¹	0.7×10 ⁻⁵ M	1.19×10 ⁻² min ⁻¹	EDTA	2.80644E-4
10mg		6.08×10 ⁻³ min ⁻¹		1.80×10 ⁻² min ⁻¹	C ₆ H ₈ O ₆	3.93772E-4
15mg		6.63×10 ⁻³ min ⁻¹		2.57×10 ⁻² min ⁻¹	NaBH ₄	3.45494E-4
pH study						
pH-11				7.10×10 ⁻³ min ⁻¹		

pH-9	$2.3 \times 10^{-5} \text{M}$	$9.10 \times 10^{-3} \text{ min}^{-1}$
pH-7		$1.06 \times 10^{-2} \text{ min}^{-1}$
pH-5		$1.56 \times 10^{-2} \text{ min}^{-1}$

Table 2: Comparative analysis of proposed study with published results on the degradation of MB

Catalyst	Dye	% removal	Time	Light Source	Ref.
Bio-CDs	Methylene Blue	94.2%	45 min	Visible light	88
N-CQDs	Methylene Blue	97%	260 min	UV light	89
TiO ₂ -CQDs	Rhodamine-B	77%	150 min	Visible light	90
NCQDs	Methylene Blue	77%	90 min	Sun light	91
NCQDs/TiO ₂	Methylene Blue	86.9%	420 min	Visible Light	92
S, N-CQDs/TiO ₂	Acid red 88	77.2	180min	Visible Light	93
CDs/TiO ₂	Methylene Blue	90%	120 min	Visible Light	94
CQDs/Bi ₂ MoO ₆	Rhodamine-B	97.1%	50 min	Solar Light	95
Cl-CQDs	Methylene Blue	56%	240 min	Solar light	96
CQDs	2-nitrophenol (2-NP)	80.79%	120 min	Sun light	97
CQDs	Methyl Orange	68.9%	120 min	Visible light	98
TiO ₂ -MCDs	Methylene Blue	83%	120 min	Visible Light	99
G-CDs	Methyl violet	63.6%	90 min	Visible light	100
luminescent carbon material	Methylene Blue	99.7%	140 min	UV light	Present work